

9-16-2008

Investigation into the $B(E2)$ Anomaly in ^{144}Nd Using Coulomb Excitation

C. R. Fitzpatrick

V. Werner

R. F. Casten

E. Williams

H. Ai

*See next page for additional authors*Follow this and additional works at: <http://scholarship.richmond.edu/physics-faculty-publications>Part of the [Nuclear Commons](#)

Recommended Citation

Fitzpatrick, C., V. Werner, R. Casten, E. Williams, H. Ai, C. Beausang, R. Cakirli, G. Gürdal, A. Heinz, E. McCutchan, D. Meyer, E. Novitski, J. Qian, and R. Winkler. "Investigation into the $B(E2)$ Anomaly in ^{144}Nd Using Coulomb Excitation." *Physical Review C* 78, no. 3 (September 16, 2008): 034309: 1-34309: 6. doi:10.1103/PhysRevC.78.034309.

This Article is brought to you for free and open access by the Physics at UR Scholarship Repository. It has been accepted for inclusion in Physics Faculty Publications by an authorized administrator of UR Scholarship Repository. For more information, please contact scholarshiprepository@richmond.edu.

Authors

C. R. Fitzpatrick, V. Werner, R. F. Casten, E. Williams, H. Ai, C. W. Beausang, R. Cakirli, G. Gurdal, A. Heinz, E. A. McCutchan, D. A. Meyer, E. Novitski, J. Qian, and R. Winkler

Investigation into the $B(E2)$ anomaly in ^{144}Nd using Coulomb excitation

C. R. Fitzpatrick,^{1,2} V. Werner,¹ R. F. Casten,¹ E. Williams,¹ H. Ai,¹ C. W. Beausang,^{1,3} R. B. Cakirli,^{1,4} G. Gürdal,^{1,5} A. Heinz,¹ E. A. McCutchan,¹ D. A. Meyer,¹ E. Novitski,¹ J. Qian,¹ and R. Winkler¹

¹WNSL, Yale University, New Haven, Connecticut 06511, USA

²University of Surrey, Guildford, Surrey GU2 7XH, United Kingdom

³University of Richmond, Richmond, Virginia 23173, USA

⁴Istanbul University, Department of Physics, Turkey

⁵Clark University, Worcester, Massachusetts 01610, USA

(Received 8 May 2008; published 16 September 2008)

The ratio of $B(E2)$ strengths between the lowest lying members of the ground state band in ^{144}Nd , $B_{4/2} = B(E2; 4_1^+ \rightarrow 2_1^+)/B(E2; 2_1^+ \rightarrow 0_1^+)$, which is used to quantify collectivity in nonmagic nuclei, has been remeasured by means of Coulomb excitation. Ambiguities in literature values for this ratio have been resolved. The results are discussed in terms of the interplay of collective and single-particle degrees of freedom, and in the context of the formation of collective structures in the $A = 140$ mass region, and more generally near (sub)shell closures. In addition, the $B_{4/2}$ ratio of ^{148}Sm has been remeasured, and the quadrupole moment of the 4_1^+ state is found to be on the order of $1 e b$.

DOI: 10.1103/PhysRevC.78.034309

PACS number(s): 21.10.Re, 25.70.De, 23.20.-g, 27.60.+j

I. INTRODUCTION

The concept of collectivity in nonmagic nuclei is one of the most fundamental findings in nuclear structure physics. Many different macroscopic models have been introduced to describe this collective behavior. Examples of such models include geometrical models depicting the atomic nucleus as a liquid drop with a given shape, and algebraic models, which only take pairs of nucleons into account. Despite the often very different approaches, all collective models have certain basic features in common, such as predictions for ratios of energies or transition rates, which have been observed in a wealth of nuclei away from closed shells.

One of the most important questions of contemporary nuclear physics is how the collective motion of nucleons arises from underlying microscopic structure. We are lacking a comprehensive understanding of how single nucleons move in distinct orbitals in a mean field potential, obey certain selection rules, and arrange themselves to show the simple patterns that we associate with rotations or vibrations of a nuclear body. Such patterns are already found in nuclei with only a few valence nucleons. Best suited to such an investigation are nuclei with low-lying structures that involve both single-particle and collective degrees of freedom.

Key observables used in assessing collectivity include the $R_{4/2}$ ratio, the ratio of the 4_1^+ and 2_1^+ state energies. $R_{4/2}$ is equal to 2 in an ideal spherical harmonic vibrator and 3.33 in an axially symmetric deformed rotor. Transition rates provide another good measure of collectivity, which is less sensitive to anharmonicities than energies. The $B(E2)$ ratio

$$B_{4/2} \equiv B(E2; 4_1^+ \rightarrow 2_1^+)/B(E2; 2_1^+ \rightarrow 0_1^+) \quad (1)$$

is a particularly good example, as it is 2 in the spherical limit and 1.4 in the deformed limit. Significant deviations from these values can be found, if one considers very small numbers of valence particles, for example, in the interacting boson model (IBM), which is discussed further in Sec. VI.

It was pointed out in Ref. [1] that a value of $B_{4/2} \leq 1$ in nonmagic nuclei is anomalously small, as it cannot be explained with collective approaches. That work also identifies other nuclei that exhibit this anomaly and suggests that their existence is a challenge for our understanding of collectivity. Inherent in this argument is the assumption that a given nucleus should exhibit enhanced collectivity. For two such nuclei, ^{98}Ru and ^{180}Pt , subsequent measurements resolved the anomalies, yielding $B_{4/2}$ values in good agreement with the spherical limit [2]. Additional evidence for $B_{4/2} \leq 1$ was obtained in the case of ^{114}Te [3], which has only two valence protons outside $Z = 50$.

With $B_{4/2} = 0.73(9)$ [4], ^{144}Nd has one of the smallest known $B_{4/2}$ values in a nonmagic nucleus and was hence listed as a possible anomalous nucleus in Ref. [1]. Similarly to ^{114}Te , it is two neutrons above the $N = 82$ shell closure. However, in contrast to ^{114}Te , the $R_{4/2}$ value of 1.89 in ^{144}Nd deviates from the collective limits as well, and hence noncollective excitations may be important.

However, with a $B(E2; 2_1^+ \rightarrow 0_1^+)$ strength of 25.9(5) W.u. [4], one could anticipate enhanced collectivity and a $B_{4/2}$ value closer to the vibrational limit. Lifetime measurements by Robinson *et al.* give $B_{4/2}^{144}\text{Nd} = 0.95(7)$ [5], which does not agree with the value adopted in the Nuclear Data Sheets (NDS) [4]. Using all data listed in the Raman compilation [6] provides a range of results; using the adopted value produces a $B_{4/2}$ ratio in between the two already quoted. The discrepancy between published values and an interest in the interplay between collective and single-particle degrees of freedom form the motivation for the present study.

The $B_{4/2}$ value of ^{144}Nd has been measured using Coulomb excitation in conjunction with cross section calculations using the code of de Boer and Winther [7]. The inclusion of ^{148}Sm , for which comprehensive lifetime information for low-lying states is available [8], in the target enabled comparison of inter- and intra-nuclear cross section ratios, thus providing an internal consistency check for the final experimental result. The resulting $B_{4/2}$ value of 0.98(3) will be discussed in Sec. VI.

in relation to other known observables for ^{144}Nd , as well as in the context of the systematic investigation of the $A = 140$ mass region, with respect to pinpointing the effects of underlying shell structure on collective structures, and the formation of collective structures.

II. PROCEDURE

Coulomb excitation is a well-established method of probing nuclear structure without involving nuclear interactions. Being an electromagnetic process, cross sections can be calculated directly and independently of nuclear models, while comparisons to observed cross sections facilitate the measurement of nuclear matrix elements [9,10]. To ensure that only pure Coulomb excitation occurs, the beam energy must be sufficiently low for the distance of closest approach to prohibit nuclear overlap. Such energies are referred to as safe energies [11].

As the quantity of interest is a ratio, a simple measurement of relative excitation yields was made, without the need for beam current integration. The following relation expresses the equivalence of excitation cross sections σ_i ($i = 1, 2$ denote two excited states) and depopulating transition intensities (I_i) when there is only one deexcitation path, as is the case for the states we are interested in, that is,

$$\frac{I_1}{I_2} = \left(\frac{\sigma_1}{\sigma_2} \right)_{\text{exp}} = \left(\frac{\sigma_1}{\sigma_2} \right)_{\text{calc}}, \quad (2)$$

where “exp” denotes data inferred from the intensity ratio and “calc” denotes values calculated using the de Boer-Winther code. The transition intensities I_i are corrected for efficiencies, feeding from higher lying states and internal conversion. A correction for angular correlations was also required because, without particle detection, a quantization axis was not defined.

In general, the derivation of matrix elements from the comparison of calculated and measured cross sections involves fitting a complete set of matrix elements to observed data. In our case, it simplifies to the variation of just one matrix element, as further discussed in Sec. IV. Once a fit is achieved, a $B_{4/2}$ value is therefore obtained.

III. EXPERIMENTAL DETAILS

A ^{48}Ti beam was delivered by the extended stretched transuranium (ESTU) tandem Van de Graaff accelerator at the Wright Nuclear Structure Laboratory (WNSL), Yale University. A beam energy of 130 MeV was chosen, which was determined experimentally to optimize the balance between population of the 4^+ state and suppression of higher lying excited states.

The target consisted of three layers: $270 \mu\text{g}/\text{cm}^2$ ^{148}Sm , $280 \mu\text{g}/\text{cm}^2$ ^{144}Nd , and $320 \mu\text{g}/\text{cm}^2$ ^{148}Sm , evaporated onto a $13.9 \text{ mg}/\text{cm}^2$ Au backing. The purpose of the backing was to stop recoils in order to minimize Doppler broadening. ^{148}Sm was chosen for inclusion in the target because it has well-known transition rate data [8] and a Coulomb barrier comparable to that of ^{144}Nd . Preliminary calculations also showed that it has similar yields compared to ^{144}Nd under the

same experimental conditions. In the triple-layer arrangement, they were subject to the same average beam energy and intensity. The original intention for ^{148}Sm was a measurement of the $4_1^+ \rightarrow 2_1^+$ and $2_1^+ \rightarrow 0_1^+$ $E2$ transition strengths in ^{144}Nd relative to those in ^{148}Sm , and the subsequent calculation of $B_{4/2}$ for ^{144}Nd . Results were instead obtained by taking ratios of observed transition rates within ^{144}Nd and ^{148}Sm . Cross-comparison of these ratios was achieved by normalization to the $2_1^+ \rightarrow 0_1^+$ transitions.

For γ -ray detection, the SPEEDY setup [12] was used, which comprises eight Compton-suppressed high-purity Ge clover detectors of the YRAST-Ball array (Yale Rochester array for spectroscopy) [13], four each in a forward ring and a backward ring, all oriented at 41.5° relative to the beam axis. Energy and efficiency calibrations were made using the most intense peaks from a ^{152}Eu source. The data were written to disk event by event. Singles data were recorded for the main analysis, along with a smaller amount of γ - γ coincidence data used to ascertain the maximum excitation energy of the nuclei of interest and to aid in the identification of contaminants.

IV. DATA ANALYSIS

Figure 1 shows the γ -ray spectrum obtained on three different scales; the upper panel illustrates the total singles spectrum, the lower panel centers on the $2_1^+ \rightarrow 0_1^+$ transitions in both ^{144}Nd and ^{148}Sm , and the inset displays the peaks corresponding to the $4_1^+ \rightarrow 2_1^+$ transitions.

Peak areas for all observed transitions in ^{144}Nd and ^{148}Sm were determined and checked for contaminants using a modified version of the RADWARE spectrum analysis program [14]. Peaks from ^{144}Nd and ^{148}Sm exhibit small Doppler tails due to recoil motion within the target (see Fig. 2). These tails were carefully incorporated into peak areas and given appropriate uncertainties. Analysis of Sm contaminants relative to ^{148}Sm revealed the intensity of their excitation to be inconsistent with the quoted isotopic enrichments for the target.

As intended, neither ^{144}Nd nor ^{148}Sm were significantly excited above the 4_1^+ state. However, the 3_1^- state in ^{148}Sm , which lies below the 4_1^+ state, was appreciably populated. Intensities from all transitions directly feeding the 2_1^+ states in both nuclei, taking into account internal conversion, were subtracted from the $2_1^+ \rightarrow 0_1^+$ intensities to ensure only Coulomb excitation of the 2_1^+ states was included in the ratio. Virtual excitation via higher lying states was found not to have a significant effect on our results.

Total excitation cross sections for the 2_1^+ and 4_1^+ states in both nuclei were calculated using the de Boer-Winther code [7]. Calculations of beam energy loss were carried out using SRIM [15] separately for each target layer, for inclusion in the Coulomb excitation calculations. The total energy loss across the target was approximately 10 MeV. Input for the calculations included transition matrix elements and level energies from the NDS [4,8], the uncertainties of which were propagated through to the final calculated cross section ratios. The matrix element that had the largest effect on the cross section ratio $\sigma(4_1^+)/\sigma(2_1^+)$ was that of the $4_1^+ \rightarrow 2_1^+$ transition,

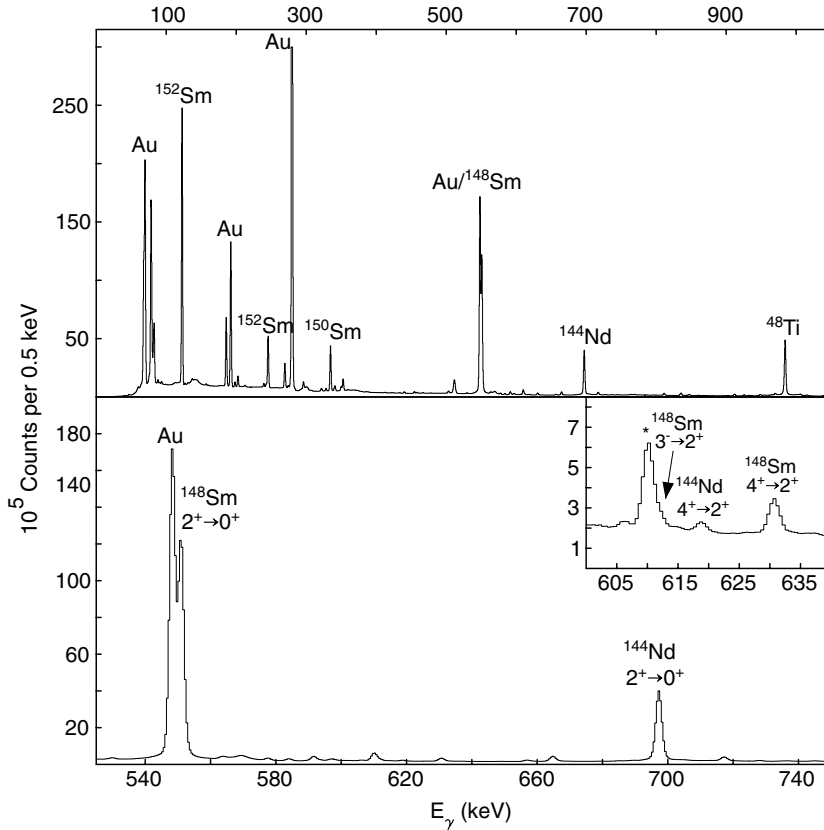


FIG. 1. γ -ray singles spectrum for 130 MeV ^{48}Ti on a $^{144}\text{Nd}/^{148}\text{Sm}$ composite target with Au backing. The dominant lines from ^{144}Nd and ^{148}Sm are labeled, as well as the main contaminants. The line at 609 keV, which almost covers the $3_1^- \rightarrow 2_1^+$ transition labeled with an asterisk, stems from ^{226}Ra , emitted by one of the bismuth germanate shield collimators. It was possible to separate both lines in the fitting process.

which was varied to fit the calculation to data. The influence of a possible one-step excitation of the 4_1^+ state was considered and found to be well within statistical errors.

Quadrupole moments were found to have a non-negligible effect on the calculated cross section ratios. When included for the 2_1^+ state in ^{148}Sm , it increased the $B_{4/2}$ ratio by 10%. As the quadrupole moment of ^{148}Sm (-0.98 ± 0.27 eb) is large enough to imply nonzero quadrupole deformation, one would also expect a significant $Q(4_1^+)$ value. However, this value is not currently known. An estimate of $Q(4_1^+) = -0.99$ eb was obtained from a fit within the interacting boson model 1 (IBM-1) [16] by Scholten *et al.* [17] and included in an additional set of cross section calculations. While no value is listed in the NDS for ^{144}Nd [4], a value of $Q(2_1^+) = -0.20 \pm 0.09$ eb was adopted. This is a weighted average of the measurements given in Refs. [18–20] and is consistent with the expected spherical symmetry of ^{144}Nd . The effect of including $Q(2_1^+)$ in calculations for ^{144}Nd on our results was less than 3%, so the effect of the unknown quadrupole moment of the 4_1^+ state was considered to be negligible.

V. RESULTS

Table I gives the cross section ratios and the resulting $B_{4/2}$ ratios obtained from the experiment using the procedure described above. The third and fourth columns give the values for ^{148}Sm without and with inclusion of the $Q(4_1^+)$ value from the IBM-1, respectively. For comparison, the cross section ratios and the $B_{4/2}$ ratios calculated from the NDS values are also given in Table I.

The $B_{4/2}$ value of ^{148}Sm obtained in this work disagrees with the listed value, unless the theoretical value for the quadrupole moment of the 4_1^+ state is included. This supports the model prediction for the quadrupole moment of the $Q(4_1^+)$ value in ^{148}Sm of 0.99 eb.

For ^{144}Nd , a value of $B_{4/2} = 0.98(3)$ was obtained. Using the literature value of $B(E2; 2_1^+ \rightarrow 0_1^+) = 25.9(5)$ W.u. [4] for

TABLE I. Results for the $B_{4/2}$ ratios of ^{144}Nd and ^{148}Sm . In the first two rows, the cross section ratios obtained from this experiment are compared with those obtained using transition strengths listed in the NDS [4,8]. The last two rows give the $B_{4/2}$ values obtained from this work and those from NDS data. For ^{148}Sm , the first column shows values obtained by only using data, and the second by including the predicted value of the $Q(4_1^+)$ quadrupole moment from the IBM-1. (Note that $Q(4_1^+)$ does not affect the measured cross section ratio.)

	^{144}Nd	^{148}Sm	$^{148}\text{Sm} (Q_{4+})^a$
$(\frac{\sigma(4_1^+)}{\sigma(2_1^+)})_{\text{this work}}$	0.0101(4)	0.0157(2)	0.0157(2)
$(\frac{\sigma(4_1^+)}{\sigma(2_1^+)})_{\text{NDS}}$	0.0079(10) ^b	0.0194(35)	0.0169(31)
$B_{4/2, \text{this work}}$	0.98(3)	1.33(4)	1.51(4)
$B_{4/2, \text{NDS}}$	0.73(9)	1.65(21)	1.65(21)

^aCalculated with the inclusion of $Q(4_1^+) = -0.99$ eb, obtained from the IBA-1 fit of ^{148}Sm [17].

^bCalculated using a weighted average of $Q(2_1^+) = -0.39(21)$ eb [18], $-0.07(15)$ eb [19], and $-0.23(15)$ eb [20].

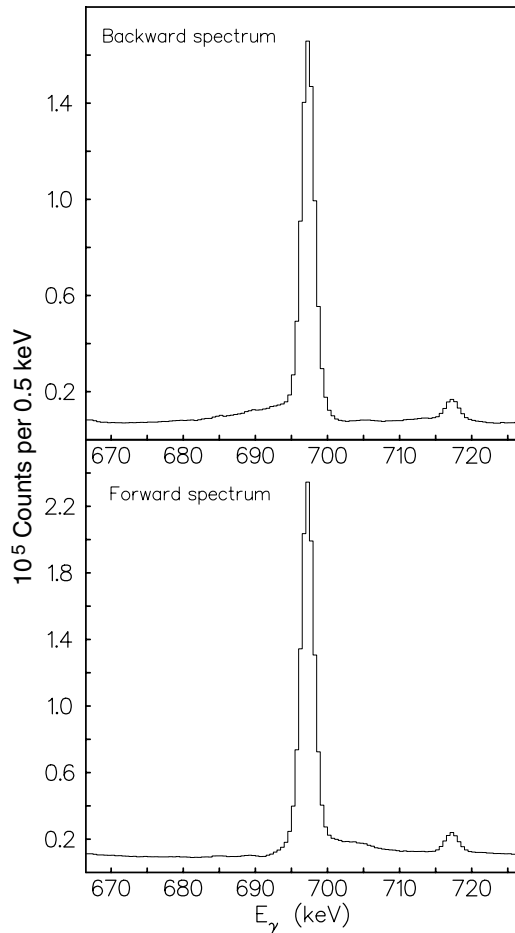


FIG. 2. Doppler-shifted peak tails. The 696 keV $2_1^+ \rightarrow 0_1^+$ transition in ^{144}Nd as recorded at forward and backward angles.

setting a scale, this results in $B(E2; 4_1^+ \rightarrow 2_1^+) = 24.5(5)$ W.u. for the decay from the 4_1^+ state.

The inclusion of ^{148}Sm in the target provided a consistency check. The ratio of the 2_1^+ cross sections in both nuclei, $\sigma(2_1^+; ^{148}\text{Sm})/\sigma(2_1^+; ^{144}\text{Nd})$, was obtained from data. Assuming that the listed lifetimes [4,8] of these states are correct, this ratio was used to extract the enrichment of ^{148}Sm in the Sm target layers, yielding about 70% enrichment in ^{148}Sm . This result was then used to extract the ratio of the 4_1^+ cross sections in both nuclei, $\sigma(4_1^+; ^{148}\text{Sm})/\sigma(4_1^+; ^{144}\text{Nd})$. Again, variation of the $4_1^+ \rightarrow 2_1^+$ matrix element in ^{144}Nd yielded a value of $B(E2; 4_1^+ \rightarrow 2_1^+) = 26(4)$ W.u., consistent with the value quoted above.

As the latter result is dependent on the absolute transition strengths of the 2_1^+ states of both isotopes, we only adopt the value of $B_{4/2}$ from the measurement within ^{144}Nd , $B_{4/2} = 0.98(3)$.

VI. DISCUSSION

The result obtained in this work is in very good agreement with that of Robinson *et al.*, $B_{4/2} = 0.95(7)$ [5], reducing the error by a factor of 2. A $B_{4/2}$ value close to unity, while larger than the ratio considered in Ref. [1], still cannot be reproduced by most collective models and requires a more microscopic

treatment. Nevertheless, ^{144}Nd exhibits a number of collective structural features; the strength of the $E2$ transition from the 2_1^+ state [25.9(5) W.u.] is indicative of a one-phonon excitation, as is the 23(5) W.u. $E3$ strength from the 3_1^- to the ground state [4].

More exotic phonon structures have been observed, mainly in photon [21,22] and neutron [23] scattering experiments. These include a one-phonon mixed-symmetry state, the quadrupole-octupole coupled two-phonon 1^- excitation, and the mixed-symmetry two-phonon 1^+ excitation, all of which are fragmented over a few states. These data are evidence of the pronounced collective features in ^{144}Nd , similar to many other vibrational nuclei in the vicinity of shell closures.

However, the $B_{4/2}$ result conflicts with collective expectations, as does the $R_{4/2}$ value of 1.89, which falls below the smallest collective model prediction. In addition, g factors within the ground state band indicate noncollective behavior [24], as they start with positive values for the 2_1^+ state, but then become negative at the 6_1^+ state. A reason for this behavior must be sought in the underlying microscopic structure of those states.

Single-particle structural influence is of particular interest around $N = 82$. In $N = 80$ nuclei, the fragmentation of the one-phonon mixed-symmetry 2^+ excitation has recently been discussed [25]. The observed fragmentation of this excitation over two states in ^{138}Ce [25] and in ^{136}Ce [26] is due to mixing with nearby symmetric states. As no such fragmentation was found in ^{136}Ba [27], it has been attributed to the closing of the proton $g_{7/2}$ orbital in the Ce isotopes [25].

If the observed fragmentation is due to a proton subshell closure at $Z = 58$ in the $N = 80$ isotones, then the same can be surmised at $N = 84$, which would affect ^{144}Nd . In fact, for ^{144}Nd a strong fragmentation of the mixed-symmetry 2^+ excitation is known from experiment [23] and was described in the quasiparticle phonon model [28]. A subshell closure at $Z = 58$, where the proton $g_{7/2}$ orbital is filled, and a shell-gap to the proton $d_{5/2}$ orbital would result in a suppression of $j = 6$ proton configurations in the 6_1^+ state of ^{144}Nd with $Z = 60$ protons. Such configurations cannot be formed with two protons within the $d_{5/2}$ orbital and require excitations from the $g_{7/2}$ orbital, as schematically shown in the bottom panel of Fig. 3, which depicts the relevant orbitals for this discussion and their occupations.

This situation would be very similar to that in the Zr isotopes at $Z = 40$. The top panel of Fig. 3 shows the relevant orbitals for ^{92}Zr in comparison with the ^{144}Nd scheme. The lowest excited 2^+ states in ^{92}Zr are predominantly formed by $j = 2$ proton and neutron configurations with seniority $\sigma = 2$ [29–31], i.e., two protons (neutrons) coupling to $j = 2$ in the same orbital. Such configurations form the building blocks of the symmetric and mixed-symmetric one-phonon 2^+ states in near-spherical even-even nuclei [27,32–34]. At $Z = 40$, the proton $p_{1/2}$ orbital closes, and for the formation of a $j = 2$ configuration protons have to be lifted across a considerable shell gap of about 700 keV to the $g_{9/2}$ orbital. This fact, in conjunction with a weak proton-neutron interaction, leads to the separation of the proton and neutron $j = 2$ configurations into two states. This effect has been introduced as configurational isospin polarization [35], a result of the

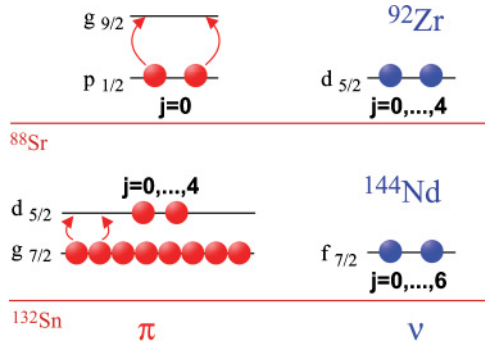


FIG. 3. (Color online) Relevant orbitals for the discussion of the low-lying states in ^{92}Zr (top panel) and ^{144}Nd (bottom panel). In ^{92}Zr , a $j = 2$ proton configuration affords an excitation of two protons to the next orbital, in contrast to the respective $j = 2$ neutron configuration. The same holds for $j = 6$ configurations in ^{144}Nd .

weak coupling of proton and neutron excitations. The effect has recently been confirmed experimentally by measuring the g factors of both states in $^{92,94}\text{Zr}$ [36,37].

At $Z = 60$, in ^{144}Nd , such configurational isospin polarization seems to appear for the first 6^+ states. The 6_1^+ state in ^{144}Nd has a negative g factor, and therefore a dominant neutron character, likely from a dominant neutron $f_{7/2}^2$ configuration. If the situation for $j = 6$ configurations in ^{144}Nd is indeed similar to that for $j = 2$ configurations in Zr isotopes, then one would expect the existence of another, higher lying 6^+ state in ^{144}Nd which is proton dominated, presumably with a dominant proton $g_{7/2}^2$ configuration.

The measured g factors in ^{144}Nd have successfully been described within a phenomenological model that couples two $f_{7/2}$ neutrons to a collective core [38]. However, a description on a more microscopic basis, especially the shell model, is still lacking. From the quasiparticle phonon model, only information on the wave functions of 2^+ states is known [28], not for the higher lying yrast states. Such calculations would be necessary to further investigate the interaction strengths involved, and may also provide insight into what inhibits the excitation of protons from the $g_{7/2}$ to the $d_{5/2}$ orbital. This is currently unclear, as no energy gap is reflected in single-particle energies. The lowest $7/2^+$ state in ^{141}Pr , corresponding to the excitation of a $g_{7/2}$ proton to the $d_{5/2}$ orbital, is found at only 145 keV excitation energy. Also, the lowest $5/2^+$ state in ^{139}La lies at 165 keV excitation energy; therefore, the shell gap can be expected to be of approximately the same size. Since the energy difference for the formation of $j = 6$ proton and neutron configurations would hence be rather small, the occurrence of configurational isospin polarization at $J^\pi = 6_1^+$ suggests an extraordinarily weak proton-neutron interaction.

The assumption that the proton $d_{5/2}$ and the neutron $g_{7/2}$ orbitals are the most relevant for the structures of the yrast states up to spin $J^\pi = 6^+$ in ^{144}Nd is supported by the large energy gap between the 6_1^+ and 8_1^+ states of 919 keV, compared with the energy difference between the 4_1^+ and 6_1^+ states of only 477 keV. This gap is due to the fact that a $j = 8$ configuration can be formed by neither the protons in the $d_{5/2}$ orbital nor the two neutrons in the $f_{7/2}$ orbital. Therefore, the structure of

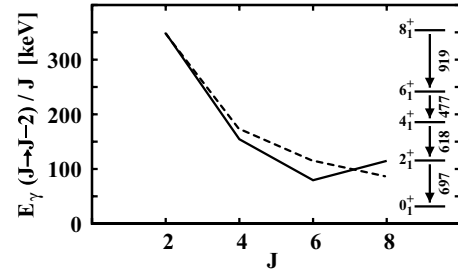


FIG. 4. E-GOS plot for the yrast states of ^{144}Nd . The solid line connects the experimental E-GOS values, the dashed line shows the harmonic vibrator expectation. The corresponding yrast level scheme, with transition energies E_γ in keV, is shown to the right.

the 8_1^+ state affords excitations to other orbitals and is quite different from the structures of the lower lying yrast states. This change in structure can be seen in Fig. 4, which shows the γ -ray energies of the decays from the yrast states $E_\gamma(J \rightarrow J - 2)$ over spin J (E-GOS [39]) as a function of J . The E-GOS values up to spin $J = 6$ gradually drop below the estimates of the harmonic vibrator, but then undergo a rise at the 8^+ state as a consequence of the change in structure.

A weakening of collectivity in ^{144}Nd is evident in the anomalous energy and $B(E2)$ ratios of the lowest states. Assuming a subshell closure at $Z = 58$ allows one to consider an IBM description in the vibrator limit [U(5)] with only two bosons, one proton and one neutron boson, corresponding to the dominating proton $d_{5/2}^2$ and neutron $f_{7/2}^2$ configurations, respectively. In this case, the first excited 2^+ and 4^+ states are formed by one- and two- d boson configurations. Even though a 6^+ state cannot be formed in such a restricted model space, and the aforementioned configurations are at most the leading configurations in the real wave functions, it is interesting that the IBM predicts a $B_{4/2}$ value of unity in this case, which is in agreement with the experimental $B_{4/2}$ value. The analytic expression for reduced $E2$ transition strengths within the ground state band in the U(5) limit is [16]

$$B(E2; J + 2 \rightarrow J) = e_B^2 \left(\frac{J + 2}{2} \right) \left(\frac{2N_B - J}{2} \right), \quad (3)$$

with the effective boson charge e_B and the boson number N_B . For $N_B = 2$, Eq. (3) yields $B_{4/2} = 1$, which is a consequence of the fact that the ground state contains no d boson, whereas the 4_1^+ state is the fully d -saturated state. The 2_1^+ and 4_1^+ states in ^{144}Nd can therefore be associated with the collective 2^+ and 4^+ one- and two-phonon states which are typical for spherical nuclei. That means that the structure of ^{144}Nd directly reflects the onset of collectivity in this mass region.

This IBM prediction for the two-boson system favors the existence of a subshell at $Z = 58$, rather than taking into account the subshell closure at $Z = 64$ (closing of the $d_{5/2}$ orbital). The latter would lead to a three-boson system, for which, according to Eq. (3), $B_{4/2} = 4/3$ in the vibrational limit. In addition, the 6_1^+ state in that case should be a three-phonon state with a g factor similar to those of the 2_1^+ and 4_1^+ states, rather than a neutron-dominated state with a negative g factor.

VII. CONCLUSIONS

Coulomb excitation was used to make a precise measurement of the $B_{4/2}$ ratio in ^{144}Nd , for which available data were ambiguous. The new result of $B_{4/2} = 0.98(3)$ is in excellent agreement with the result of Robinson *et al.* [5], clarifying the extent to which this value deviates from collective expectations. These data, in conjunction with lifetime and g -factor measurements, reflects the closing of the proton $g_{7/2}$ orbital. The precise determination of the $B_{4/2}$ ratio will be important to constrain future microscopic analysis of this region, where features of a subshell closure are more strongly observed

than would be expected from single-particle energies alone, possibly as a result of very weak proton-neutron coupling.

ACKNOWLEDGMENTS

The authors would like to thank N. Pietralla, P. Regan, and A. Garnsworthy for fruitful discussions, as well as N. Benczer-Koller for help with the Coulomb excitation code, A. Lipski for the supply of targets, and the WNSL operations team for providing the beam. This work was supported by the U.S. DOE under Grant Nos. DE-FG02-91ER40609, DE-FG52-06NA26206, and DE-FG02-88ER40417.

-
- [1] R. B. Cakirli, R. F. Casten, J. Jolie, and N. Warr, *Phys. Rev. C* **70**, 047302 (2004).
- [2] E. Williams, C. Plettner, E. A. McCutchan, H. Levine, N. V. Zamfir, R. B. Cakirli, R. F. Casten, H. Ai, C. W. Beausang, G. Gürdal *et al.*, *Phys. Rev. C* **74**, 024302 (2006).
- [3] O. Möller, N. Warr, J. Jolie, A. Dewald, A. Fitzler, A. Linnemann, K. O. Zell, P. E. Garrett, and S. W. Yates, *Phys. Rev. C* **71**, 064324 (2005).
- [4] A. A. Sonzogni, *Nucl. Data Sheets* **93**, 599 (2001).
- [5] S. J. Robinson, B. Faircloth, P. Miočinović, and A. S. Altgilbers, *Phys. Rev. C* **62**, 044306 (2000).
- [6] S. Raman, J. C. W. Nestor, and P. Tikkanen, *At. Data Nucl. Data Tables* **78**, 1 (2001).
- [7] A. Winther and J. de Boer, *Tech. Rep.*, California Institute of Technology, 1965.
- [8] M. R. Bhat, *Nucl. Data Sheets* **89**, 797 (2000).
- [9] K. Alder and A. Winther, *Phys. Rev.* **96**, 237 (1954).
- [10] K. Alder, A. Bohr, T. Huus, B. Mottelson, and A. Winther, *Rev. Mod. Phys.* **28**, 432 (1956).
- [11] R. E. Neese and M. W. Guidry, *Phys. Rev. C* **25**, 881 (1982).
- [12] R. Krücken, in *Proceedings of the International Symposium on Advanced Nuclear Physics*, edited by D. Poenaru and S. Stoica (World Scientific, Singapore, 2000), p. 336.
- [13] C. W. Beausang, C. J. Barton, M. A. Caprio, R. F. Casten, J. R. Cooper, R. Krücken, B. Liu, J. R. Novak, Z. Wang, M. Wilhelm *et al.*, *Nucl. Instrum. Methods Phys. Res. A* **452**, 431 (2000).
- [14] D. C. Radford, RADWARE analysis package (unpublished), modified by M. Caprio.
- [15] J. F. Ziegler, J. P. Biersack, and U. Littmark, *The Stopping Range of Ions in Solids* (Pergamon, New York, 1985).
- [16] F. Iachello and A. Arima, *The Interacting Boson Model* (Cambridge University Press, Cambridge, 1987).
- [17] O. Scholten, F. Iachello, and A. Arima, *Ann. Phys. (NY)* **115**, 325 (1978).
- [18] P. A. Crowley, J. R. Kerns, and J. X. Saladin, *Phys. Rev. C* **3**, 2049 (1971).
- [19] H. S. Gertzman, D. Cline, H. E. Grove, and P. M. S. Lesser, *Nucl. Phys.* **A151**, 282 (1971).
- [20] J. B. Gupta, *Nucl. Phys.* **A484**, 189 (1988).
- [21] T. Eckert, O. Beck, J. Besserer, P. von Brentano, R. Fischer, R.-D. Herzberg, U. Kneissl, J. Margraf, H. Maser, A. Nord *et al.*, *Phys. Rev. C* **56**, 1256 (1997).
- [22] T. Eckert, O. Beck, J. Besserer, P. von Brentano, R. Fischer, R.-D. Herzberg, U. Kneissl, J. Margraf, H. Maser, A. Nord *et al.*, *Phys. Rev. C* **57**, 1007 (1998).
- [23] S. F. Hicks, C. M. Davoren, W. M. Faulkner, and J. R. Vanhoy, *Phys. Rev. C* **57**, 2264 (1998).
- [24] J. Holden, N. Benczer-Koller, G. Jakob, G. Kumbartzki, T. J. Mertzimekis, K.-H. Speidel, A. Macchiavelli, M. McMahan, L. Phair, P. Maier-Komor *et al.*, *Phys. Lett.* **B493**, 7 (2000).
- [25] G. Rainovski, N. Pietralla, T. Ahn, C. J. Lister, R. V. F. Janssens, M. P. Carpenter, S. Zhu, and C. J. Barton III, *Phys. Rev. Lett.* **96**, 122501 (2006).
- [26] T. Ahn, N. Pietralla, G. Rainovski, A. Costin, K. Dusling, T. C. Li, A. Linnemann, and S. Pontillo, *Phys. Rev. C* **75**, 014313 (2007).
- [27] N. Pietralla, D. Belic, P. von Brentano, C. Fransen, R.-D. Herzberg, U. Kneissl, H. Maser, P. Matschinsky, A. Nord, T. Otsuka *et al.*, *Phys. Rev. C* **58**, 796 (1998).
- [28] C. Stoyanov, N. L. Iudice, N. Tsoneva, and M. Grinberg, *Phys. At. Nucl.* **64**, 1223 (2001).
- [29] A. Holt, T. Engeland, M. Hjorth-Jensen, and E. Osnes, *Phys. Rev. C* **61**, 064318 (2000).
- [30] V. Werner, D. Belic, P. von Brentano, C. Fransen, A. Gade, H. von Garrel, J. Jolie, U. Kneissl, C. Kohstall, A. Linnemann *et al.*, *Phys. Lett.* **B550**, 140 (2002).
- [31] C. Fransen, V. Werner, D. Bandyopadhyay, N. Boukharouba, S. R. Leshner, M. T. McEllistrem, J. Jolie, N. Pietralla, P. von Brentano, and S. W. Yates, *Phys. Rev. C* **71**, 054304 (2005).
- [32] A. Arima, T. Otsuka, F. Iachello, and I. Talmi, *Phys. Lett.* **B66**, 205 (1977).
- [33] K. Heyde and J. Sau, *Phys. Rev. C* **33**, 1050 (1986).
- [34] N. Pietralla, C. Fransen, D. Belic, P. von Brentano, C. Frießner, U. Kneissl, A. Linnemann, A. Nord, H. H. Pitz, T. Otsuka *et al.*, *Phys. Rev. Lett.* **83**, 1303 (1999).
- [35] J. D. Holt, N. Pietralla, J. W. Holt, T. T. S. Kuo, and G. Rainovski, *Phys. Rev. C* **76**, 034325 (2007).
- [36] G. Jakob, N. Benczer-Koller, J. Holden, G. Kumbartzki, T. J. Mertzimekis, K.-H. Speidel, C. W. Beausang, and R. Krücken, *Phys. Lett.* **B468**, 13 (1999).
- [37] V. Werner, N. Benczer-Koller, G. Kumbartzki, J. D. Holt, P. Boutachkov, E. Stefanova, M. Perry, N. Pietralla, H. Ai, K. Aleksandrova *et al.*, *Phys. Rev. C* (R) (in press).
- [38] J. Copnell, S. J. Robinson, J. Jolie, and K. Heyde, *Phys. Rev. C* **46**, 1301 (1992).
- [39] P. H. Regan, C. W. Beausang, N. V. Zamfir, R. F. Casten, J. ye Zhang, A. D. Yamamoto, M. A. Caprio, G. Gürdal, A. A. Hecht, C. Hutter *et al.*, *Phys. Rev. Lett.* **90**, 152502 (2003).